

Transitions in function at low Reynolds number: hair-bearing animal appendages

M. A. R. Koehl*

Department of Integrative Biology, University of California, Berkeley, CA 94720-3140, U.S.A.

SUMMARY

Many types of animals use appendages bearing arrays of hair-like structures to capture molecules (e.g. olfactory antennae, gills) or particles (e.g. suspension-feeding appendages) from the surrounding water or air, and to locomote or move fluid past themselves. The performance of these functions depends on how much of the fluid encountered by the array of hairs flows through the gaps between the hairs rather than around the perimeter of the whole array. By modelling such arrays of hairs as rows of finite width of cylinders operating at low Reynolds numbers, the fluid velocity fields with respect to the hairs were calculated. Such models revealed a transition from non-leaky to leaky behaviour as Re was increased. The purpose of this paper is to provide a brief review of the features of this transition as revealed by models, and then to describe examples of how animals use the transition in fluid flow to perform particular functions: rejection of captured material by copepods, and sniffing by lobsters. Copyright © 2001 John Wiley & Sons, Ltd.

KEY WORDS: biofluidynamics; copepod; aesthetasc

1. INTRODUCTION

Many diverse animals use appendages bearing arrays of hair-like structures to perform a variety of important biological functions (reviewed in References [1,2]). Some of these functions involve mass exchange with the surrounding water or air, such as the capture of molecules by gills or by olfactory antennae, or the capture of particulate food by suspension-feeding appendages. Other functions performed by feathery or bristly appendages involve momentum exchange with the surrounding fluid. For example, flapping setulose appendages can create feeding or ventilatory currents past an animal, while hairy legs can propel small animals through the water and hairy wings can be used by tiny insects to fly. To understand how hair-bearing structures perform these important biological functions, we must work out how arrays of small, hair-like cylinders interact with the fluid around them.

*Correspondence to: M. A. R. Koehl, Department of Integrative Biology, University of California, Berkeley, CA 94720-3140, U.S.A.

Contract/grant sponsor: Office of Naval Research; grant numbers: N00014-98-0775, N00014-97-1-026; John D. and Catherine T. MacArthur Foundation Fellowship

Mathematical and physical modelling revealed a transition in the fluid flow around and through rows of cylinders that depends on the size, spacing, and speed of the cylinders relative to the fluid. The purpose of this paper is to provide a brief review of the features of this transition as revealed by models, and then to describe several examples of how animals use the transition in fluid flow to perform particular functions.

2. MODELS OF FLUID FLOW NEAR HAIRS IN AN ARRAY

The Reynolds numbers of the little hairs on the suspension-feeding, locomotory, and olfactory appendages listed above range from 10^{-5} to 10 (reviewed in References [3–7]). The Reynolds number of a hair ($Re = UL/\nu$, where U is velocity, L is hair diameter, and ν is the kinematic viscosity of the fluid) represents the ratio of inertial to viscous forces determining the fluid motion around the hair. Viscosity is very important in determining flow patterns at these low Re 's, although inertia cannot be ignored for hairs operating at the upper end of this Re range.

One approach to modelling the fluid motion relative to hairs in a row of finite width is to consider the simplest case, a pair of cylinders. Cheer and Koehl [5] calculated fluid velocities between and around a pair of circular cylinders at low Re using a two-dimensional model. Fluid velocities far from the cylinders were calculated in polar co-ordinates using Oseen's low- Re approximation of the Navier–Stokes equation (which includes inertial effects), while fluid velocities near the cylinders were calculated in bipolar coordinates using Stoke's low- Re approximation. The flow field between and around the cylinders was produced using a matched asymptotic expansion technique. The model of Cheer and Koehl has also been used to estimate the flow through feathery appendages composed of hairs that bear bristles [8–10]. The velocity profile between neighbouring hairs was calculated to determine the velocities encountered at defined positions along the length of bristles on these hairs; then these local velocities were used as the freestream velocities in calculations of velocity profiles between adjacent bristles. Because the model described in Cheer and Koehl [5] only deals with two cylinders at $Re \leq 0.5$, Abdullah and Cheer (unpublished; described in Reference [9]) used a numerical model to compute the steady, two-dimensional flow near cylinders at Re 's between 0.5 and 4 and investigated the consequences of adding more cylinders to a row.

Various other approaches have been used to calculate fluid motion through a filter or hairy appendage. Such a structure can be modelled as an infinite row of cylinders (e.g. References [11–15]) or as a porous plate (e.g. References [16–18, 8]). Comparisons of model results with measurements of fluid flow through hair-bearing appendages [8] and through physical models of such appendages [19, 20, 1] suggest that the model of Cheer and Koehl [5] yields much better matches with empirical observations than do the other models (except in the case of arrays of cylinders that form screens, such as the silk feeding nets spun by aquatic caddisfly larvae [21]).

3. A TRANSITION IN FLUID FLOW AT LOW REYNOLDS NUMBER

When a hair moves through a viscous fluid, a velocity gradient develops in the fluid around the hair because the layer of fluid in contact with the hair's surface does not slip relative to the hair. The layer of sheared fluid moving along with the hair becomes thicker relative to the

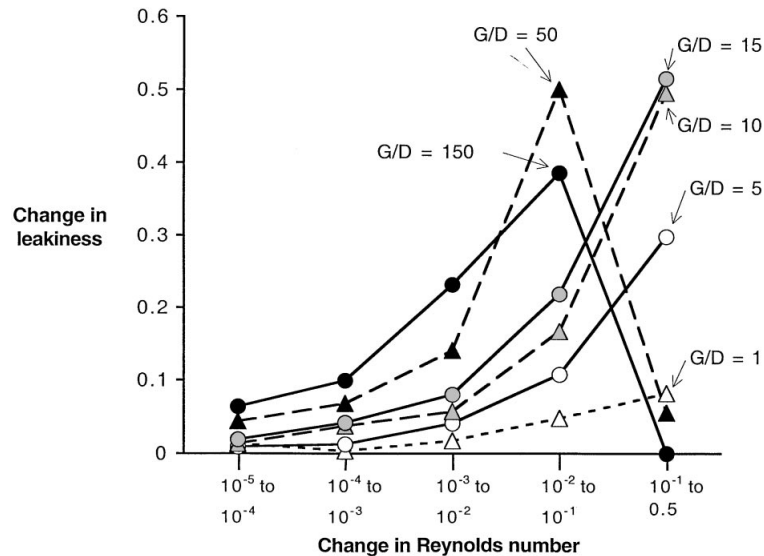


Figure 1. The change in leakiness produced by a change in Reynolds number. Leakiness (defined in the text) was calculated using the model of Cheer and Koehl [5]. Different symbols represent cylinders with different spacings (G = gap width between neighbouring cylinders; D = cylinder diameter).

diameter of the hair if the Re is lowered. If the layers of fluid moving along with the hairs in an array are thick relative to the gaps between the hairs, then little fluid may leak through the array. The 'leakiness' of a gap between neighbouring hairs in an array is defined as the ratio of the volume of fluid that flows through the gap in a unit of time to the volume of fluid that would flow at freestream velocity through a space of that width if there were no hairs present [5]. If the leakiness of a hair-bearing appendage is high, the appendage functions like a sieve. In contrast, if the leakiness of a row of hairs on a structure is low, then the structure functions like a paddle, even though it is full of holes between neighbouring hairs.

By integrating the velocity profiles calculated using the model of Cheer and Koehl [5], we determined the leakiness of pairs of hairs operating at a variety of biologically relevant Re 's and spacings (hair spacing is described by the ratio of the width of the gap, G , between neighbouring hairs to the diameter, D , of a hair). We found that, at a Re of 0.5, little fluid is dragged along with the cylinders as they move, and leakiness is quite high if G/D is ≥ 5 . Therefore, appendages whose hairs operate in this Re and G/D range should function like leaky sieves. In contrast, we found that, at $Re \leq 10^{-3}$, little fluid moves through the gap between adjacent cylinders, even when G/D is very high. Thus, appendages whose hairs operate at such low Re 's should behave like paddles. These calculations [5] reveal that a transition in the function of an array of hairs, between operating like a solid paddle and functioning like a leaky sieve, occurs as Re is changed.

The change in leakiness produced by a change in Re is plotted in Figure 1. A change in Re can represent either a change in the velocity with which an organism moves an appendage (i.e. an alteration in behaviour), or a change in the diameter of the hairs (i.e. an ontogenetic change in the size of an individual, or an evolutionary change in the size of members of different taxa in a lineage). At very low Re , changes in speed or hair diameter have little

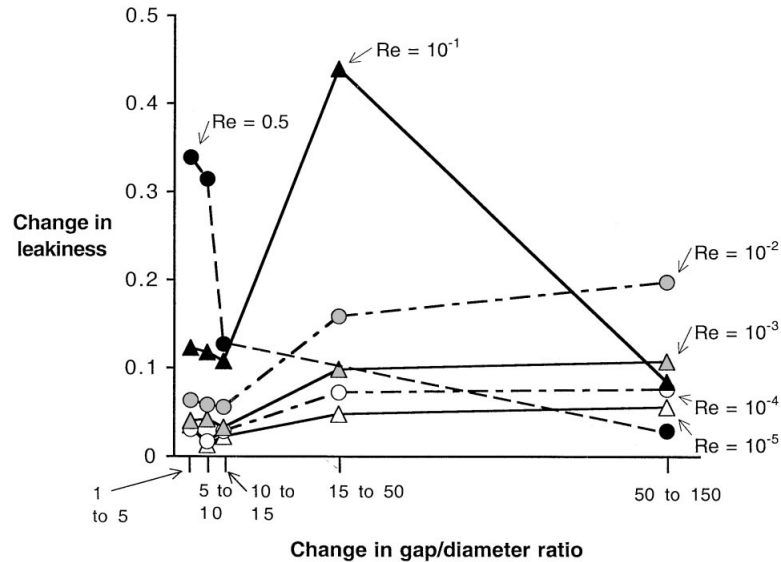


Figure 2. The change in leakiness produced by a change in the spacing of neighbouring cylinders (G = gap width between neighbouring cylinders; D = cylinder diameter). Leakiness (defined in the text) was calculated using the model of Cheer and Koehl [5]. Different symbols represent cylinders operating at different Reynolds numbers (Re), calculated using cylinder diameter as the linear dimension.

effect on leakiness, so we should expect permission in this Re range for diversity in the size and speed of hairy appendages without consequences to performance that depends on leakiness. In contrast, at higher Re 's, a transition between sieve- and paddle-like behaviour occurs as Re is changed. The more widely spaced the hairs, the lower the Re range in which this transition occurs.

The change in leakiness produced by a change in the spacing (G/D) of the hairs in an array is shown in Figure 2. At very low Re , G/D has little effect on leakiness, whereas at Re 's $\geq 10^{-2}$, G/D can make a big difference to leakiness. The higher the Re , the lower the G/D range in which the leakiness transition occurs. For example, at Re of order 10^{-1} , the leakiness of appendages with widely spaced hairs (G/D 's around 50) should be sensitive to changes in hair spacing, whereas at Re of order 1, only appendages with very closely spaced hairs ($G/D \leq 10$) are sensitive to changes in hair spacing.

Physical and numerical models of arrays of cylinders have provided more information about the transition in fluid flow through hair-bearing appendages. For example, Leonard [19] and Hansen and Tiselius [20] measured flow through comb-like physical models at Re 's up to ~ 40 , higher than those at which the mathematical model of Cheer and Koehl [5] is applicable. These physical models revealed that leakiness is very sensitive to hair spacing only when hairs are very close together at Re 's of order 10, and that the critical G/D below which gap width affects leakiness becomes lower as Re is increased [1]. Another example is provided by the model of Abdullah and Cheer (unpublished; described in Reference [9]), which predicts that the addition of more hairs to a row reduces leakiness if $Re < 1$, but has the opposite effect and increases leakiness if $Re > 1$. This transition in the consequences to leakiness of increasing hair number was also noted in experiments involving physical models (reviewed in Reference

[1]). The hair-bearing appendages of animals generally operate near solid boundaries, such as the surface of the animal's body. Loudon *et al.* [7] measured the leakiness of pairs of cylinders towed towards or parallel to a wall. At $Re \geq 10^{-1}$, we found that the wall made little difference to leakiness, whereas at $Re \leq 10^{-2}$, we discovered that movement near a wall increased leakiness. Thus, there is a transition in the type of behaviour that affects leakiness as Re is changed: at very low Re 's, moving an appendage bearing an array of hairs close to the body surface can increase leakiness, whereas at Re 's approaching 1, changing appendage speed can alter leakiness.

Thus, models of flow through rows of finite width of cylinders operating at low Re have revealed a transition from non-leaky to leaky behaviour as Re is increased. These models led us to predict that animal appendages bearing arrays of hairs might switch between paddle-like and sieve-like function if they change their speed of motion in the critical hair Re range at which the transition in leakiness occurs.

4. BIOLOGICAL EXAMPLES

Fluid movement around and through arrays of hairs on animal appendages has been studied using various experimental and theoretical approaches. Using high-speed cinematography or videography of animals as they flap their hair-bearing appendages, we can measure the kinematics of the hairs on the appendages as well as the velocities of fluid markers moving relative to them (e.g. References [22, 9, 1, 23]). Morphometric measurements such as hair diameters can be made using light or scanning electron micrographs of the appendages. These kinematic and morphometric parameters can then be used to calculate the small-scale velocity profiles around individual hairs (e.g. References [8–10]). Alternatively, velocity profiles around individual hairs can be measured using particle image velocimetry of dynamically scaled physical models of the appendages. If a model and a real appendage are geometrically similar and operate at the same Re , they are dynamically similar and the ratios of velocities and forces at analogous points in the fluid around the model and the appendage are the same. For example, a large model, moved at a conveniently slow speed in a high-viscosity Newtonian fluid, can be used to study the fluid dynamics of a microscopic appendage operating at the same Re in water or air (e.g. References [1, 2, 24, 25]).

Such studies of the hair-bearing appendages of a variety of diverse animals have revealed cases in which the appendages operate as leaky sieves versus others in which the appendages function like non-leaky paddles, even though they are full of holes (e.g. References [1, 2, 9, 10, 24, 25]). In a number of cases, the array of hairs on an animal appendage operates in the Re range in which its leakiness is especially sensitive to changes in appendage velocity. I will describe two such appendages, copepod second maxillae and lobster antennules, to illustrate how changes in velocity and the consequent changes in leakiness can enhance appendage function.

4.1. Rejection of unwanted materials by feeding copepods

Calanoid copepods are small planktonic crustaceans (body lengths of a few mm) that can be very abundant in oceans and lakes. Many copepods eat single-celled algae and thus often are a critical link in aquatic food webs between the phytoplankton and higher trophic levels (such as

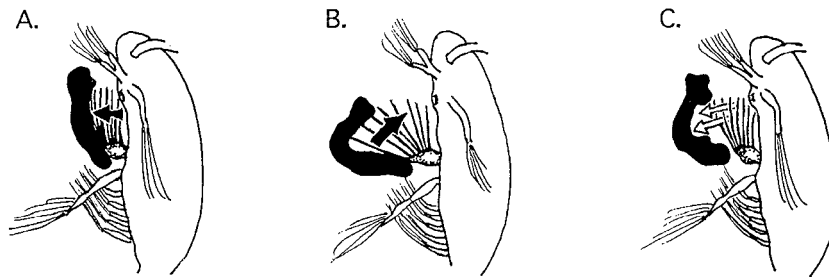


Figure 3. Diagram of a side view of a copepod, *Eucalanus pileatus*, rejecting a blob of dye (drawn in black). The diagram was produced by tracing frames of a movie of the animal (details described in Reference [22]). Only the left M2 is shown in the drawing. (A) The M2's scrape along the body surface and collect the dye on the outside of their array of hairs, and then the M2's move away from the body surface in the direction indicated by the black arrow. The dye does not flow between the hairs of the M2 during the outward motion (i.e. the M2's are not leaky). (B) After the unwanted material has been pushed away from the animal's body by the M2's, they move more rapidly back towards the body surface in the direction indicated by the black arrow. (C) Water flows between the hairs of the M2's during the leaky motion towards the body (water flow direction with respect to the hairs of the M2 is indicated by white arrows). This water separates the material being rejected from the M2's. The discarded material is then carried away from the copepod in the 'scanning current' of water past the animal that is produced by the flapping of other appendages (e.g. [22,32,1]).

fish). Because copepod feeding is so important ecologically, many studies measuring copepod feeding rates and selectivity have been conducted (reviewed e.g. in References [26–30]). To complement these studies, we have been investigating the physical mechanisms copepods use to catch particles such as single-celled algae.

High-speed microcinematography of seawater labelled with dye and released from micropipettes near the animals while they were catching food particles revealed the appendage and water motions involved in feeding by a number of species of copepods ([22,1,24], Koehl and Paffenhöfer, unpubl. data). The last stage in particle capture is performed by a pair of appendages, the second maxillae (M2's), that catch particles by flinging apart from each other and then squeezing back together again. Each M2 is composed of a row of long hairs (called 'setae') that bear smaller barbs (called 'setules'); the coarseness of this mesh of hairs differs between species, as does the Re range in which the setae operate (e.g. References [1,9,24]).

Eucalanus pileatus is a species of copepod that is very plastic in its feeding behaviour. For example, they catch individual large algal cells with a single fling-and-squeeze of their M2's, but propel small algal cells towards their mouths with a series of low-amplitude flaps of their M2's ([22,31], Koehl and Paffenhöfer, unpubl. data). During these feeding motions, the setae of *E. pileatus* M2's operate at Re 's of order 10^{-2} . Both mathematical models (Cheer, unpublished results reviewed in [9]) and dynamically scaled physical models [1] indicate that *E. pileatus* M2's have very low leakiness and function as paddles during such feeding motions.

If feeding *E. pileatus* catch material they do not want, they reject it using a special behaviour of their M2's [22]. The M2's scrape along the body surface and collect the unwanted material on the outside of the setal array. The M2's move away from the body surface, carrying the unwanted material (Figure 3(A)); the M2's then move back towards the body

surface more rapidly, leaving the rejected material behind (Figure 3(B) and 3(C)), where it is carried away in a water current produced by other appendages of the copepod. Calculations (using the technique described in Reference [8] for hairs bearing bristles) of the flow profiles around setae bearing setules of the sizes and spacings of those of *E. pileatus* M2's indicate that the M2's have a low leakiness during the slow outstroke of this rejection behaviour, but become leakier during the more rapid instroke (Cheer, unpublished results, reviewed in [9]). Thus, an *E. pileatus* can push unwanted material away from its body using slowly moving, paddle-like M2's; the M2's can then move away from that material during the more rapid inward motion when water flows through the leaky hair arrays on the M2's. At the Re 's at which the rejection behaviour occurs, the motion of the M2's towards the body surface should further increase their leakiness [7]. This transition in leakiness can be observed in movies of *E. pileatus* rejecting water labelled with dye (Figure 3).

Experiments in which physical models of M2's of a variety of species of copepods were moved at various Re 's, suggested that *E. pileatus* conduct their rejection behaviour in a range of Re 's in which the leakiness transition occurs. The model experiments revealed that such a transition in leakiness occurred at slower speeds (lower Re 's) for M2's that were more coarsely meshed (i.e. had a larger G/D for both setae and setules) than those of *E. pileatus*, and occurred at higher speeds (higher Re 's) for M2's that were more finely meshed than those of *E. pileatus* [1].

4.2. Sniffing by lobsters

Chemical cues in the water or air around an animal can provide important information about the environment, such as the location of food or conspecifics. Many animals capture odour molecules from the surrounding fluid using olfactory antennae that bear arrays of microscopic hairs containing chemosensory neurons (e.g. References [33–35]). The leakiness of an array of olfactory hairs can affect molecule interception in two ways: (1) the volume of water or air that can be filtered per time depends on how easily fluid can penetrate the array of hairs; and (2) the steepness of the velocity gradients near individual hairs affects the flux of molecules to the surfaces of the hairs (e.g. References [36–39,2]).

Crustaceans such as lobsters, mantis shrimp, and crabs, capture odour molecules with the chemosensory hairs (aesthetascs) on the lateral branches of their antennules, which they flick through the surrounding water (reviewed in e.g. [40,2]). It has been suggested that antennule flicking is a mechanism of increasing the flow of water (and the odour molecules it carries) into the array of aesthetascs (e.g. [41–46]). Although models of molecule interception by a single cylinder show that changes in flow velocity have a relatively small effect on the rate of interception of odour molecules by the cylinder [36,38], models of arrays of cylinders predict that changes in flow velocity can have a large effect on the rate of molecule capture by a sensory hair in that array *if* the velocity change occurs in the Re range in which the leakiness of that array of hairs is sensitive to Re [39].

We investigated the fluid motion around versus through the aesthetasc arrays of the antennules of spiny lobsters, *Panulirus argus*. Using high-speed video analysis of lobster antennules, we determined that the Re of the aesthetascs was 2 during the rapid flick downstroke, whereas the Re was only 0.5 during the slower upstroke [47]. Measurements of the fluid flow around a dynamically scaled physical model of the lateral branch of a *P. argus* antennule [2] revealed that fluid moves through the array of closely spaced aesthetascs during the leaky downstroke,

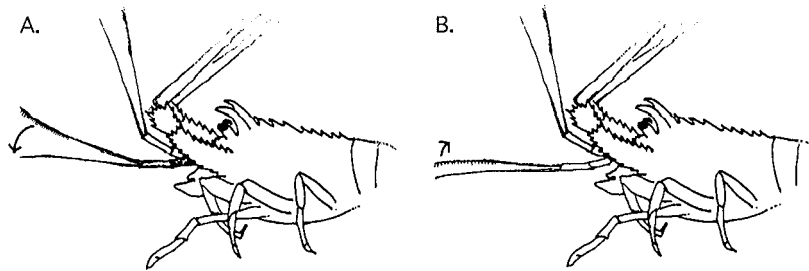


Figure 4. Side view of the anterior end of a spiny lobster, *Panulirus argus*, flicking the lateral branch of its left olfactory antennule. The lateral branch bears an array of olfactory hairs near its distal end. (A) The arrow indicates the direction of movement of the lateral branch of the antennule during the downstroke of the flick. (B) The arrow indicates the direction of movement of the lateral branch during the slower upstroke of the flick.

but flows around the array during the slower, non-leaky upstroke. Furthermore, planar laser-induced fluorescence measurements of fluid penetration into aesthetasc arrays of real *P. argus* antennules flicking in ambient water currents in a flume ([2]; Koehl, Koseff, Cooper, McCay, Crimaldi, and Wiley, unpublished data) also showed that water readily penetrates the array during the flick downstroke, but not during the upstroke or during pauses between flicks when the antennule is stationary with its long axis pointing roughly upstream (as it would be when the animal faces upstream in an odour plume). Thus, during the leaky downstroke, 'old' water is flushed out of the aesthetasc array and replaced by a 'new' water sample, which is essentially retained within the aesthetasc array during the upstroke and the pause between flicks. Thus, because *P. argus* antennules operate at this critical range of aesthetasc Re 's in which leakiness is very sensitive to speed, they are able to take discrete water samples in space and time with each flick, akin to sniffing (Fig. 4).

5. CONCLUSIONS

Both mathematical and physical models of fluid velocity profiles around cylinders in rows of finite width show that a transition in the leakiness of an array of cylinders occurs as the Re of the cylinders or the width of the gap between them is changed. The more widely spaced the cylinders in an array (i.e. the greater the G/D), the lower the Re at which the transition occurs between non-leaky paddle-like behaviour and leaky sieve-like function. These models led us to predict that animal appendages bearing arrays of hairs might switch between paddle-like and sieve-like function if they change their speed of motion in the critical hair Re range at which the transition in leakiness occurs. The particle-capturing second maxillae of calanoid copepods and the molecule-capturing olfactory antennules of lobsters provide examples of how organisms can use the change in leakiness produced by a change in appendage speed to perform particular functions.

ACKNOWLEDGEMENTS

This research was supported by a grant from the Office of Naval Research, U.S.A. (N00014-98-0775), by an Augmentation Award for Science and Engineering Research Training (N00014-97-1-026), and by a fellowship from the John D. and Catherine T. MacArthur Foundation. I am grateful to D. Abdullah, B. Best, A. Cheer, T. Cooper, J. Crimaldi, J. Goldman, W. Hu, J. Jed, J. Koseff, C. Loudon, M. McCay, G. Paffenhöfer, R. Strickler, G. Wang, and M. Wiley for collaborating on various aspects of the work cited here.

REFERENCES

1. Koehl MAR. Fluid flow through hair-bearing appendages: Feeding, smelling, and swimming at low and intermediate Reynolds number. In *Biological Fluid Dynamics*, Ellington CP, Pedley TJ (eds.). *Society of Experimental Biology Symposium* 1995; **49**:157–182.
2. Koehl MAR. Fluid dynamics of animal appendages that capture molecules: arthropod olfactory antennae. In *Conference Proceedings of the IMA Workshop on Computational Modeling in Biological Fluid Dynamics*, Gueron S, Fauci L (eds.), 2001; **124**: in press.
3. Rubenstein DI, Koehl, MAR. The mechanisms of filter feeding: some theoretical considerations. *American Naturalist* 1977; **111**:981–994.
4. LaBarbera M. Feeding currents and particle capture mechanisms in suspension feeding animals. *American Zoologist* 1984; **24**:71–84.
5. Cheer AYL, Koehl MAR. Paddles and rakes: fluid flow through bristled appendages of small organisms. *Journal of Theoretical Biology* 1987; **129**:17–39.
6. Shimeta J, Jumars PA. Physical mechanisms and rates of particle capture by suspension-feeders. *Oceanography and Marine Biology Annual Reviews* 1991; **29**:191–257.
7. Loudon C, Best BA, Koehl MAR. When does motion relative to neighboring surfaces alter the flow through an array of hairs? *Journal of Experimental Biology* 1994; **193**:233–254.
8. Cheer AYL, Koehl MAR. Fluid flow through filtering appendages of insects. *International Mathematics Association Journal of Mathematics and Applied Medical Biology* 1987; **4**:185–199.
9. Koehl MAR. Hairy little legs: feeding, smelling, and swimming at low Reynolds number. *Contemporary Mathematics* 1993; **141**:33–64.
10. Loudon C, Koehl MAR. Sniffing by a silkworm moth: wing fanning enhances air penetration through and pheromone interception by antennae. *Journal of Experimental Biology* 2000; **203**:2977–2990.
11. Tamada K, Fujikawa H. The steady two-dimensional flow of viscous fluid at low Reynolds numbers passing through an infinite row of equal parallel circular cylinders. *Quarterly Journal of Mechanics and Applied Mathematics* 1957; **10**:425–432.
12. Fuchs NA. *The Mechanics of Aerosols*. Pergamon: New York, 1964.
13. Davies CN. *Air Filtration*. Academic Press: New York, 1973.
14. Laws EM, Livesay JL. Flow through screens. *Annual Reviews in Fluid Mechanics* 1978; **10**:247–266.
15. Silvester NR. Some hydrodynamic aspects of filter feeding with rectangular-mesh nets. *Journal of Theoretical Biology* 1983; **103**:265–286.
16. Taylor GI, Batchelor GK. The effects of wire gauze on small disturbances in uniform stream. *Quarterly Journal of Mechanics and Applied Mathematics* 1949; **10**:1–29.
17. Spielman L, Goren SL. Model for predicting pressure drop and filtration efficiency in fibrous media. *Environmental Science and Technology* 1968; **2**:279–287.
18. Koo J-K, James DF. Fluid flow around and through a screen. *Journal of Fluid Mechanics* 1973; **60**:513–538.
19. Leonard ABP. The biomechanics, autecology and behavior of suspension-feeding in crinoid echinoderms. *Ph.D. Dissertation*, University of California, San Diego, 1992.
20. Hansen B, Tiselius P. Flow through the feeding structures of suspension feeding zooplankton: a physical model approach. *Journal of Plankton Research* 1992; **14**:821–834.
21. Loudon C. Empirical test of filtering theory: particle capture by rectangular-mesh nets. *Limnology and Oceanography* 1990; **35**:134–148.
22. Koehl MAR, Strickler, JR. Copepod feeding currents: Food capture at low Reynolds number. *Limnology and Oceanography* 1981; **26**:1062–1073.
23. Mead KS, Koehl MAR, O'Donnell MJ. Stomatopod sniffing: the scaling of chemosensory sensillae and flicking behavior with body size. *Journal of Experimental Marine Biology and Ecology* 1999; **241**:235–261.
24. Koehl MAR. Small-scale hydrodynamics of feeding appendages of marine animals. *Oceanography* 1998; **11**: 10–12.
25. Mead KS, Koehl MAR. Stomatopod antennule design: the asymmetry, sampling efficiency, and ontogeny of olfactory flicking. *Journal of Experimental Biology* 2000; **203**:3795–3808.

26. Koehl MAR. Mechanisms of particle capture by copepods at low Reynolds numbers: possible modes of selective feeding. In *Trophic Dynamics Within Aquatic Ecosystems*, Meyers DG, Strickler JR (eds.). Westview Press: Boulder, CO, 1984; 135–166.
27. Kleppel GS. On the diets of calanoid copepods. *Marine Ecology—Progress Series* 1993; **99**:183–195.
28. Hansen B, Bjornsen PK, Hansen PJ. The size ratio between planktonic predators and their prey. *Limnology and Oceanography* 1994; **39**:395–403.
29. Harris RP. Feeding ecology of *Cananus*. *Ophelia* 1996; **44**:85–109.
30. Naganuma T. Calanoid copepods: Linking lower-higher trophic levels by linking lower-higher Reynolds numbers. *Marine Ecology—Progress Series* 1996; **136**:311–313.
31. Price HJ, Paffenhöfer G-A. Capture of small cells by the copepod *Eucalanus elongatus*. *Limnology and Oceanography* 1986; **31**:189–194.
32. Childress S, Koehl MAR, Miksis M. Scanning currents in Stokes flow and the efficient feeding of small organisms. *Journal of Fluid Mechanics* 1987; **177**:407–436.
33. Zacharuk RY. Antennae and sensilla. In *Comprehensive Insect Physiology, Biochemistry and Pharmacology*, Kerkut GA, Gilbert LI (eds.). Pergamon Press: New York, 1985; 1–69.
34. Grünert U, Ache BW. Ultrastructure of the aesthetasc (olfactory) sensilla of the spiny lobster, *Panulirus argus*. *Cell Tissue Research* 1988; **251**:95–103.
35. Hallberg E, Johansson KUI, Elofsson R. The aesthetasc concept: Structural variations of putative olfactory receptor cell complexes in crustacea. *Microscopic Research Techniques* 1992; **22**:325–335.
36. Adam G, Delbruk M. Reduction in dimensionality in biological diffusion processes. In *Structural Chemistry and Molecular Biology*, Rich A, Davidson, N (eds.). Freeman and Co.: San Francisco, 1968; 198–215.
37. Berg HC, Purcell EM. Physics of Chemoreception. *Biophysics Journal* 1977; **20**:193–219.
38. Murray JD. Reduction of dimensionality in diffusion processes: antenna receptors of moths. In *Nonlinear Differential Equation Models in Biology*. Oxford University Press: Oxford, 1977; 83–127.
39. Koehl MAR. Small-scale fluid dynamics of olfactory antennae. *Marine and Freshwater Behaviour and Physiology* 1996; **27**:127–141.
40. Atema J. Chemical signals in the marine environment: dispersal, detection, and temporal signal analysis. In *Chemical Ecology: The Chemistry of Biotic Interaction*, Eisner T, Meinwald J (eds.). National Academy Press: Washington, DC, 1995; 147–159.
41. Snow PJ. The antennular activities of the hermit crab, *Pagurus alaskensis* (Benedict). *Journal of Experimental Biology* 1973; **58**:745–765.
42. Schmidt BC, Ache BW. Olfaction: responses of a decapod crustacean are enhanced by flicking. *Science* 1979; **205**:204–206.
43. Atema J. Chemoreception in the sea: adaptations of chemoreceptors and behavior to aquatic stimulus conditions. *Society of Experimental Biology Symposium* 1985; **39**:3423–3887.
44. Moore PA, Gerhardt GA, Atema J. High resolution spatio-temporal analysis of aquatic chemical signals using microchemical electrodes. *Chemical Senses* 1989; **14**:829–840.
45. Moore PA, Atema J, Gerhardt GA. Fluid dynamics and microscale chemical movement in the chemosensory appendages of the lobster, *Homarus americanus*. *Chemical Senses* 1991; **16**:663–674.
46. Gleeson RA, Carr WES, Trapido-Rosenthal HG. Morphological characteristics facilitating stimulus access and removal in the olfactory organ of the spiny lobster, *Panulirus argus*: insight from the design. *Chemical Senses* 1993; **18**:67–75.
47. Goldman JA, Koehl MAR. Fluid dynamic design of lobster olfactory organs: high-speed kinematic analysis of antennule flicking by *Panulirus argus*. *Chemical Senses*, in press.